



ARTICLE

DNA methylation episignature and comparative epigenomic profiling of *HNRNPU*-related neurodevelopmental disorder



ARTICLE INFO

Article history:

Received 19 January 2023

Received in revised form

24 April 2023

Accepted 24 April 2023

Available online 28 April 2023

Keywords:

CNV

DNA methylation

Episignature

HNRNPU

Neurodevelopmental disorder

ABSTRACT

Purpose: *HNRNPU* haploinsufficiency is associated with developmental and epileptic encephalopathy 54. This neurodevelopmental disorder is characterized by developmental delay, intellectual disability, speech impairment, and early-onset epilepsy. We performed genome-wide DNA methylation (DNAm) analysis in a cohort of individuals to develop a diagnostic biomarker and gain functional insights into the molecular pathophysiology of *HNRNPU*-related disorder.

Methods: DNAm profiles of individuals carrying pathogenic *HNRNPU* variants, identified through an international multicenter collaboration, were assessed using Infinium Methylation EPIC arrays. Statistical and functional correlation analyses were performed comparing the *HNRNPU* cohort with 56 previously reported DNAm episignatures.

Results: A robust and reproducible DNAm episignature and global DNAm profile were identified. Correlation analysis identified partial overlap and similarity of the global *HNRNPU* DNAm profile to several other rare disorders.

Conclusion: This study demonstrates new evidence of a specific and sensitive DNAm episignature associated with pathogenic heterozygous *HNRNPU* variants, establishing its utility as a clinical biomarker for the expansion of the EpiSign diagnostic test.

© 2023 American College of Medical Genetics and Genomics.

Published by Elsevier Inc. All rights reserved.

Introduction

HNRNPU (heterogeneous nuclear ribonucleoprotein U; OMIM 602869) haploinsufficiency has been associated with a neurodevelopmental disorder (NDD) referred to as developmental and epileptic encephalopathy 54 (DEE54; OMIM 617391).^{1,2} DEE54 is characterized by developmental delay and intellectual disability (ID)—typically moderate to severe—with speech and language delay and/or absent speech. Affected individuals may also display autistic

features. There may be feeding difficulties during the neonatal period, as well as hypotonia, which often remains lifelong. Dysmorphic features have been described but they are nonspecific. Affected individuals are likely to experience seizures (most commonly tonic-clonic or absence) that may be refractory to treatment. Nonspecific brain magnetic resonance imaging (MRI) findings include ventriculomegaly and thinning of the corpus callosum. Less common findings include cardiac abnormalities, strabismus, undescended testes in males, renal anomalies, and skeletal features,

The Article Publishing Charge (APC) for this article was paid by Peter Henneman.

Kathleen Rooney and Liselot van der Laan contributed equally to this work.

Bekim Sadikovic, Mieke M. van Haelst, and Peter Henneman are senior authors contributed equally to this work.

*Correspondence and requests for materials should be addressed to Bekim Sadikovic, Department of Pathology and Laboratory Medicine, Western University, 1151 Richmond St, London, ON N6A 3K7, Canada. *Email address:* bekim.sadikovic@lhsc.on.ca OR Peter Henneman, Department of Human Genetics, Amsterdam Reproduction & Development Research Institute, Amsterdam University Medical Centers, University of Amsterdam, Meibergdreef 9, 1105 AZ, Amsterdam, The Netherlands. *Email address:* p.henneman@amsterdamumc.nl

A full list of authors and affiliations appears at the end of the paper.

doi: <https://doi.org/10.1016/j.gim.2023.100871>

1098-3600/© 2023 American College of Medical Genetics and Genomics. Published by Elsevier Inc. All rights reserved.

including joint laxity, polydactyly, and scoliosis. Rarely, abnormal breathing patterns, including hyperventilation and apnea, may be present and can lead to sleep disturbance.¹⁻⁵

Heterogeneous nuclear ribonucleoproteins (HNRNPs) are part of an RNA-binding protein family containing multiple extraordinarily complex and versatile proteins that are involved in the control of the maturation of newly formed nuclear RNAs into messenger RNAs. They also play a role in RNA splicing, polyadenylation, capping, modification, export, localization, translation, and turnover.³ In addition, HNRNPs have interactions with other ribonucleoproteins (RNPs) and are directly involved in every stage of messenger RNA processing and formation; hence, they are essential in early development.⁴ The observed high variety of HNRNP functions results from multiple different alternatively spliced isoforms that form many distinct protein complexes with other *HNRNP* genes.⁵ As successful RNA regulation is important in all cell types, many *HNRNPs* have also been linked to other diseases, such as spinal muscular atrophy, amyotrophic lateral sclerosis, congenital myasthenic syndrome, multiple sclerosis, Alzheimer disease, and frontotemporal lobe dementia.⁵⁻⁷ It is observed that *HNRNPU* is the largest among the HNRNP proteins and forms a complex capable of organizing and stabilizing nuclear chromatin, regulating gene transcription, RNA splicing, and RNA stability.⁵⁻⁷ It has also been shown that *HNRNPU* regulates topologically associated domain boundaries, which are linked to the three-dimensional chromatin organization and functions in epigenetic regulation.⁸

Genes involved in epigenetic machinery have been categorized as readers, writers, erasers, and remodelers.⁹ The phenotypes that result from aberrations linked to the epigenetic machinery are mostly associated with ID, delayed growth, and with or without dysmorphic features.^{9,10} Epigenetic regulators have critical roles during embryonic and fetal development. Germline variants in genes involved in the epigenetic machinery can result in distinct DNA methylation (DNAm) patterns referred to as episignatures.¹¹

Given its role in chromatin organization and regulation,¹⁰ we hypothesized that individuals with pathogenic *HNRNPU* variants would exhibit a specific DNAm episignature. DNAm episignature assessment using the EpiSign classifier can detect more than 56 episignatures associated with 65 disorders.¹² Copy number variant (CNV) syndromes, such as the 22q11.2 deletion syndrome, have also demonstrated a unique episignature.¹³ CNVs are variable in size and may involve multiple genes. The clinical outcome of CNVs can therefore be the result of the combined effects of disturbances of multiple genes, some of which have been shown to influence the global DNAm patterns, ultimately episignatures, in patients.^{14,15} Episignature mapping and assessment by EpiSign can be applied in genome diagnostics to reclassify previously identified variants of uncertain significance (VUS) in genes with defined episignatures, and EpiSign can detect imprinting disorders, such as Angelman and Beckwith-Wiedemann syndromes.¹⁶ Of note, *DEE54* can be difficult to diagnose because it is

characterized by a broad and often nonspecific range of clinical features.¹⁷ Furthermore, current ClinVar database contains >240 entries of VUS in the *HNRNPU* gene (<https://www.ncbi.nlm.nih.gov/clinvar>) highlighting the need for development of functional assays to enable accurate molecular diagnosis in this disorder.

In this study, we aimed to (1) find a DNAm episignature in patients with heterozygous pathogenic single-nucleotide *HNRNPU* variants or deletions spanning *HNRNPU*, (2) validate this episignature using an independent set of cases with pathogenic variants and *HNRNPU* VUS, and (3) compare the global DNAm profiles associated with *HNRNPU* with previously described episignatures.

Materials and Methods

Subjects and study cohort

The study cohort includes 10 individuals (7 males and 3 females) with *HNRNPU* variants, 4 of which (cases 3, 4, 8, and 9) have been previously described.^{2,18,19} All individuals were identified in a clinical diagnostic setting. Variants have been identified through chromosome microarray analysis (CMA), exome sequencing (ES), or targeted gene panels and were classified according to the guidelines of the American College of Medical Genetics (ACMG) and Association for Molecular Pathology.^{20,21} Eight individuals were identified with a likely pathogenic/pathogenic *HNRNPU* variant: (1) 4 had frameshift variants, (2) 2 had large deletions including *HNRNPU*, as well as several other genes, (3) 1 had a deletion limited to *HNRNPU* only, (4) and 1 had a splice-site variant. In addition, we included 1 case with an in-frame deletion in *HNRNPU* classified as a VUS (case 9) and a previously unresolved case (case 10). Case 10 was submitted previously for EpiSign testing as a first-line diagnostic test, solely based on the clinical phenotype. This analysis, however, did not yield any conclusive result, and the profile was added to our EpiSign Knowledge Database (EKD), annotated as an unresolved case. For the in-frame deletion, bioinformatic protein structure analyses were based on different in silico tools: SIFT,²² MutPred-indel score,²³ and mutation taster.²⁴

Methylation analysis

DNA isolation from peripheral blood was performed according to standard techniques. DNA methylation analysis on the DNA samples were carried out using the Illumina Infinium methylation EPIC bead chip arrays according to manufacturer's protocols. Analysis and discovery of episignatures were carried out based on our laboratory's previously published protocols.^{12,25,26} In brief, intensity data files containing methylated and unmethylated signal intensities were analyzed in R (version 4.1.1). Methylation data normalization was performed using the Illumina normalization method with background

correction using the minfi package (version 1.40.0) in R.²⁷ The following probes were eliminated: probes with detection P value $> .1$, probes located on chromosomes X and Y, probes containing single-nucleotide polymorphism at or near the CpG interrogation or single-nucleotide extension sites, and probes that cross react with other genomic regions. Probes with beta values of 0 and 1, and the top 1% most variable probes were removed. DNA methylation assessment was performed 3 times; twice for epesignature detection in biomarker discovery and once to assess the global *HNRNPU* DNAm profile as described in the results. Principal component analysis was performed each time to examine batch structure and identify case or control outliers. Matched controls were randomly selected at a ratio of 1:5 from the EKD,¹⁶ matched by age, sex, and array type using the MatchIt package (version 4.3.4).²⁸ Methylation levels for each probe (beta values) were converted to M-values by logit transformation and subsequently applied in linear regression analysis (limma package, v3.50.0) to identify differentially methylated probes (DMPs).²⁹ Estimated blood cell proportions were incorporated into the model matrix as confounding variables.³⁰ P values were moderated using the eBayes function in the limma package.²⁹

Probe selection and training of the machine classifier

Selection of probes for the discovery and final epesignatures was performed in 3 steps. First, 900 and 1000 probes, respectively, were retained with the highest product of absolute methylation differences between cases and controls and the negative of the logarithm of P values. This was followed by a receiver's operating characteristic curve analysis, in which 450 and 333 probes were retained with the highest area under the receiver's operating characteristic curve. Probes with pairwise correlation greater than 0.65 and 0.70 measured using Pearson correlation coefficients for all probes were eliminated. Unsupervised clustering models were applied using the remaining probes, including hierarchical clustering (heatmap) using Ward's method on Euclidean distance in the ggplot2 package in R (v3.1.1) and multidimensional scaling (MDS) by scaling of the pairwise Euclidean distances between samples. To assess the robustness of the epesignatures, multiple rounds of leave-1-out cross validation were performed: in each round, a single *HNRNPU* sample was used as a testing sample and the remainder used for probe selection. The corresponding unsupervised clustering plots were visualized. The e1071 R package (version 1.7-9) was used to train a support vector machine (SVM) classifier and to construct a binary prediction model as previously described.^{12,25}

Assessment of differentially methylated regions

Differentially methylated regions (DMRs) were detected using the DMRcate package in R (v 2.8.3), with probability-cutoff set to default (false discovery rate).³¹ Regions

containing at least 5 significantly different CpGs within 1 kb, with a minimum mean methylation difference of 5% and a Fisher's multiple comparison P value $< .01$ were considered significant. Of note, DMRs were annotated using the UCSC Genome Browser Data Integrator with GENCODE V3lift37 comprehensive annotations (<https://genome.ucsc.edu>) and further characterized using the following UCSC Genome Browser tracks: UCSC Genes, CpG Islands (CGIs), H1-hESC Genome Segmentation by Combined Segway+ChromHMM selection from the Genome Segments track, and the H3K27Ac Mark from the ENCODE regulation track.

Functional annotation of the global *HNRNPU* DNAm profile and correlation to the 56 NDD epesignatures on EpiSign

Functional annotation and EpiSign cohort comparisons were performed according to our previously published methods.²⁶ In short, heatmaps and circos plots were produced to assess the percentage of DMPs shared between the *HNRNPU* epesignature and the 56 other NDD epesignatures on the EpiSign clinical classifier. Heatmaps were plotted using the R package heatmap (version 1.0.12) and circos plots using the R package circlize (version 0.4.15).³² To investigate relationships across all 57 cohorts without bias because of the number of DMPs selected, clustering analysis was performed on the combined top N DMPs for each cohort as described previously by Levy et al.²⁶ This assessed the top 500 DMPs for each cohort, ranked by P value. For cohorts with less than 500 DMPs, all DMPs were used. The distance and similarities between cohorts were visualized on a tree and leaf plot. Tree and leaf plots were generated using the R package TreeAndLeaf (version 1.6.1) showing additional information, including global mean methylation difference and total number of DMPs identified for each cohort.

To determine the genomic location of the DMPs, probes were annotated in relation to CGIs and genes using the R package annotator (version 1.20.0)³³ with AnnotationHub (version 3.2.2) and annotations hg19_cpgs, hg19_basicgenes, hg19_genes_intergenic, and hg19_genes_intronexonboundaries. In addition, CGI annotations included CGI shores from 0 to 2 kb on either side of CGIs, CGI shelves from 2 to 4 kb on either side of CGIs, and inter-CGI regions encompassing all remaining regions. For gene annotations, promoters included up to 1 kb upstream of the transcription start site (TSS) and promoter+ the region 1 to 5 kb upstream of the TSS. Annotations to untranslated regions (5'-UTR and 3'-UTR), exons, introns, and exon/intron boundaries were combined into the "gene body" category. A chi-squared goodness of fit test was performed in R to assess the significance between background DMP annotation distribution and the *HNRNPU* cohort annotation distribution. P values were obtained for both annotation categories: genes and CGIs.

Results

Identification and assessment of the *HNRNPU* epismature

The molecular details of our study cohort are summarized in [Table 1](#) and [Figure 1](#). All individuals carried an *HNRNPU* variant or large CNV, including *HNRNPU*.

Clinical summary

The clinical details of our cohort are summarized in [Table 2](#) and [Figure 2](#) (more detailed reports in Supplemental information including classification scores).^{20,21} All patients presented with ID, language delay, and facial dysmorphism.

Case 1

This female was referred to the clinical geneticist at 11 months of age for evaluation of hypotonia, gait disturbance, and seizures ([Figure 2A](#) and [B](#)). She also had pyelonephritis with vesicoureteral reflux and a right-sided double collecting system. Electroencephalography recorded multifocal epileptic abnormalities. An MRI of the brain showed a very prominent sagittal sinus and Computed tomography scan of the brain revealed a hypoplastic jugular foramen. In addition, ID gene panel sequencing showed a pathogenic NM_031844.2:c.906_907del p.(Asp304Serfs*33) *HNRNPU* variant.

Case 2

This 28-year-old male was referred to the clinical geneticist for evaluation of his ID ([Figure 2C](#)). Previous medical history mentioned intrauterine growth restriction and feeding difficulties. A ventriculo-peritoneal drain was placed at 3 months of age as treatment of hydrocephalus. At 15 years of age, this individual was treated by percutaneous epiphysodesis of the right knee because of a leg length discrepancy. Also, MRI of the brain showed hydrocephalus, possibly due to aqueductal stenosis and a periventricular cyst, possibly post-hemorrhagic. In addition, ID gene panel sequencing showed a pathogenic NM_031844.2:c.216_2478+8418del p.(?) *HNRNPU* variant.

Case 3

This 28-year-old male was referred to the clinical geneticist at 21 years of age for evaluation of ID and generalized tonic-clonic seizures. ES showed a likely pathogenic NM_031844.2:c.2425-3C>A p.(?) *HNRNPU* variant.

Case 4

This 11-year-old female was referred to the clinical geneticist at 15 months of age for evaluation of ID and tonic-clonic generalized seizures with an abnormal electroencephalogram (EEG) ([Figure 2D](#)). Brain MRI revealed mild enlargement of the third and lateral ventricles. Because of short stature and reduced growth hormone secretion after

stimulation tests with arginine and glucagon, she was started on growth hormone replacement therapy at 10 years of age. ES revealed a pathogenic NM_031844.2:c.2304_2305del p.(Gly769Glu fs*83) *HNRNPU* variant.

Case 5

This 20-year-old male was referred the clinical geneticist at 8 years of age for evaluation of ID and microcephaly. CMA showed a pathogenic CNV arr(GRCh37) 1q43q44(242045197_249212668)x1 including *HNRNPU*.

Case 6

This case was referred to a clinical geneticist at 3 years because of a profound global developmental delay and epilepsy ([Figure 2E](#)). In his neonatal period he showed hypotonia, at 15 months had febrile seizures, and at 3 years was diagnosed with epilepsy (generalized tonic-clonic) refractory to many antiepileptic drugs. His medical history is positive for cryptorchidism, as well as pectus carinatum and kyphoscoliosis. He is non-verbal and has a slow gait but can walk autonomously. At 17 years, his CMA revealed a pathogenic de novo arr[GRCh37] 1q43q44(244571975_246704522)x1 CNV involving *HNRNPU*.

Case 7

This 29-year-old male was referred to the clinical geneticist at 17 years of age for evaluation of ID, seizures, and epilepsy ([Figure 2F](#) and [G](#)). His medical history noted a heart murmur that was detected after birth, as well as a VSD/ASD on ultrasound. ID gene panel sequencing showed a likely pathogenic NM_031844.2:c.2072del p.(Asn691Ilefs*143) *HNRNPU* variant. The variant was not maternal, and the father was not tested; therefore, we assume this variant is likely de novo.

Case 8

This 14-year-old female was first referred to a pediatric neurology at 2 months of age because of seizures and hypotonia ([Figure 2H](#) and [I](#)). Later she was referred to the clinical geneticist at 6 years of age for evaluation of ID and febrile seizures. An MRI of the brain revealed enlarged lateral ventricles and white matter hypotrophy. Also, ES showed a likely pathogenic NM_031844.2:c.16delinsATT, p.(Val6Ilefs*4) *HNRNPU* variant. The variant was identified in father in a mosaic state.

Case 9

This 17-year-old male was referred to the clinical geneticist at 15 years of age for evaluation of ID, seizures, and dysmorphic features. Also, ES revealed a VUS in *HNRNPU*: NM_031844.2:c.837_839del p.(Glu279del).

Case 10

This 3-year-old male was referred to the clinical genetics at 2 years and 11 months of age for ID, facial dysmorphism, and hypotonia. An MRI indicated prominent perivascular spaces and a mildly abnormal dens. Also, ID gene panel sequencing

Table 1 HNRNPU variants detected in cases 1 to 10

Case	ClinVar SCV Code	Cohort Type	Variant Type	Genomic Change	Nucleotide Change	Amino Acid Change	Classification	Inheritance	Test
1	SCV002774882	Discovery	Frameshift	g.245023747_245023748del	c.906_907 del	p.(Asp304Serfs*33)	P	dn	Trio genpanel
2	SCV002774884	Discovery	In-frame deletion	g.245017752_245035812del	c.216_2478+8418del	large gene deletion	P	dn	ID panel
3	SCV002774885	Discovery	Splice	g.245017808G>T	c.2425-3C>A	p.(?)	LP	dn	ES
4	SCV002774887	Discovery	Frameshift	g.245018775_245018776del	c.2304_2305del	p.(Gly769Glufs*83)	P	dn	ES
5	SCV002774889	Discovery	Deletion	g.242045197_249212668del	arr[GRCh37] 1q43q44 (242045197_249212668)x1	full gene deletion	P	dn	CMA
6	SCV002774890	Discovery	Deletion	g.244571975_246704522del	arr[GRCh37] 1q43q44 (244571975_246704522)x1	full gene deletion	P	dn	CMA
7	SCV002774886	Validation	Frameshift	g.245019302del	c.2072del	p.(Asn691Ilefs*143)	LP	Probably dn ^a	ID panel
8	SCV002774888	Validation	Frameshift	g.245027594del _245027594insAAT	c.16delinsATT	p.(Val6Ilefs*4)	LP	Paternal mosaicism	ES
9	SCV002774891	Validation _VUS	In-frame deletion	g.245025809_245025811del	c.837_839del	p.(Glu279del)	VUS	dn	ES
10	SCV002774883	Unresolved case	In-frame deletion	g.245020054_245020056del	c.1720_1722del	p.(Lys574del)	LP	dn	ES

Variants are based on (NM_031844.2).

CMA, chromosome micro array; dn, de novo; ES, exome sequencing; ID, intellectual disability; LP, likely pathogenic; P, pathogenic; VUS, variant of uncertain significance

^aFather not tested.

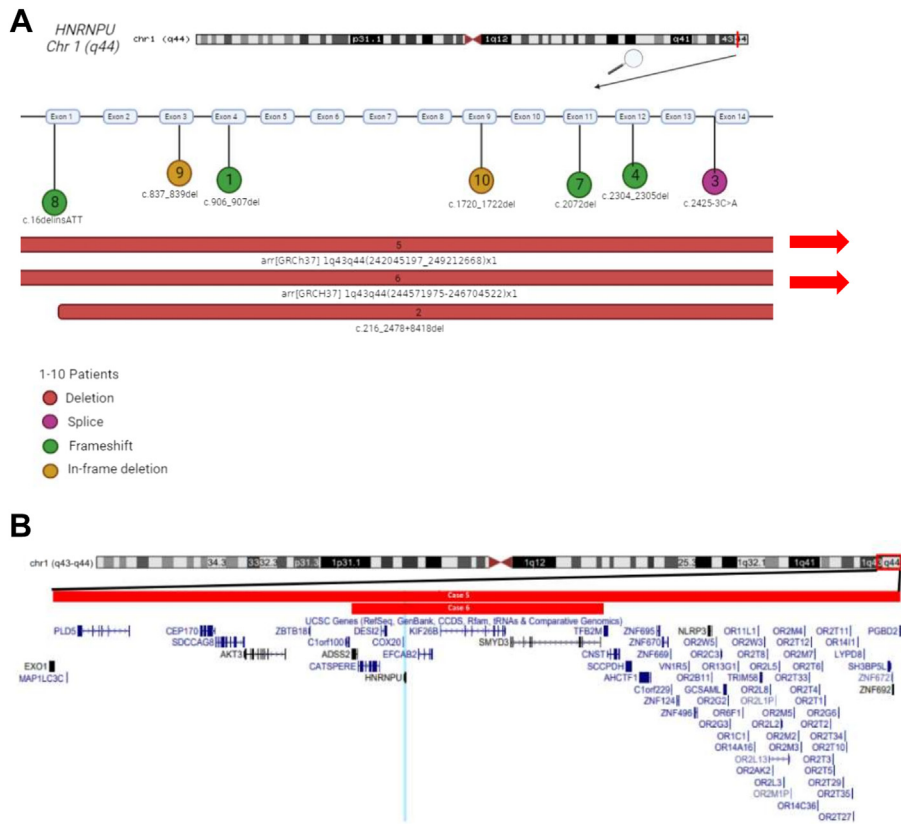


Figure 1 Molecular characterization of *HNRNPU* variants. A. Molecular information of cases 1 to 10 of the *HNRNPU* cohort. All variants are nonrecurrent. The numbers match the numbers in the table and figures. Comparison between the individuals with deletions (red bar), splice (purple circle), frameshift (green circle), and in-frame deletion (yellow circle) variants. Alamut Visual version NM_031844.2 *HNRNPU*. The arrows at the end of the CNVs of cases 5 and 6 indicate that they are larger and extend beyond the current window view. Created with BioRender.com. B. Large deletions of chromosome region 1q43q44 in cases 5 and 6 are represented by the horizontal red bars and the genes contained within the region listed below. Also highlighted in light blue is the location of *HNRNPU*. Cytogenetic bands and known genes are presented in this figure using the UCSC Genome Browser 2009 (GRCh37/hg19) genome build.³⁴ CNV, copy number variant.

showed a likely pathogenic NM_031844.2:c.1720_1722del p.(Lys574del) *HNRNPU* variant.

Identification of a DNAm epismature

We set out to determine if individuals with pathogenic variants in *HNRNPU* would exhibit a unique and specific DNAm pattern compared to unaffected controls. Epismature analysis identified 123 differentially methylated CpG probes that successfully distinguished between *HNRNPU* cases and unaffected controls (Supplemental Table 1). Unsupervised clustering methods, specifically hierarchical clustering (heatmap) and MDS methods confirmed that *HNRNPU* cases clustered apart from unaffected controls based on differential methylation at the selected probes (Figure 3A and B). Next, based on multiple rounds of leave-one-out cross validation, we observed a robust epismature, which was visualized by heatmap and MDS plots (Figure 3A and B, Supplemental Figure 1). Next, we constructed an SVM classifier model, including 56 other NDD epismatures, which indicated a high level of specificity of the *HNRNPU* epismature. Herein, all *HNRNPU*

cases showed a methylation variant pathogenicity (MVP) score close to 1, compared with all 56 others that showed an MVP score at or close to 0 (Figure 3C).

Validation of the *HNRNPU* epismature and assessment of a VUS

To validate the *HNRNPU*-associated epismature, we evaluated 2 additional cases with likely pathogenic variants in this gene (cases 7 and 8) and an individual carrying the NM_031844.2:c.837_839del p.(Glu279del) VUS (case 9) as testing cases. We visualized these results using unsupervised hierarchical and MDS clustering methods. We confirmed that both samples carrying pathogenic variants clustered with the *HNRNPU* epismature training cases and away from controls (Figure 4A and B). In contrast, the assessment of the case carrying a VUS in *HNRNPU* (case 9) showed that it did not cluster with the epismature cases. Indeed, a reevaluation of NM_031844.2:c.837_839del p.(Glu279del) (case 9) showed 2 cases with the same variant in the Genome Aggregation Database (gnomAD ver 2.1.1), as well as discordant pathogenic in silico predictions (SIFT:

Table 2 Clinical details of the HNRNPU cohort

Case	1	2	3	4	5	6	7	8	9	10
General information										
Sex	F	M	M	F	M	M	M	F	M	M
Age (y)	6	31	28	11	20	28	29	14	17	3
Clinical information										
Age at assessment (y)	11 m	28	21	11	8	28	17	6	15	2 y 11 m
Microcephaly	–	–	–	+	+	–	NA	+	–	–
Macrocephaly	–	+	–	–	–	–	NA	–	–	–
Behavior										
Intellectual disability	+	+	+	+	+	+	+	+	+	+
Developmental delay	+	+	+	–	+	+	+	+	+	+
Motor delay	+	+	+	–	+	+	+	+	+	+
Language delay	+	+	+	+	+	+	+	+	+	+
Behavior abnormalities	+	+	NA	+	NA	–	+	–	–	+
Autistic features	+	+	+	–	NA	–	+	NA	–	+
ASD diagnosis	–	NA	NA	–	NA	–	+	–	NA	–
Neurologic symptoms										
Hypotonia	+	+	–	–	NA	+	+	+	–	+
Gait disturbance	+	NA	NA	–	NA	–	+	NA	–	NA
Seizures	+	+	–	+	NA	+	+	+	+	–
Epilepsy	+	+	+	+	NA	+	+	+	+	–
MRI abnormalities	+	+	NA	+	NA	–	+	+	–	+
Dysmorphism										
Craniofacial dysmorphism	+	+	+	–	NA	+	+	+	+	+
Bulbous nasal tip	+	–	+	+	NA	+	NA	+	–	–
Anteverted nares	+	–	+	–	NA	+	NA	–	–	+
Short nose	+	–	+	+	NA	–	NA	+	–	+
Hypertelorism	NA	–	+	–	NA	–	NA	+	–	–
Deep-set eyes	+	+	+	–	NA	–	NA	–	–	+
Limbs/hands	NA	+	+	+	NA	–	NA	–	+	+
Other										
Cardiac anomalies	NA	–	–	–	NA	–	+	+	NA	–
Musculoskeletal anomalies	NA	+	NA	–	NA	+	NA	+	NA	–
Dental anomalies	NA	+	–	–	NA	+	+	NA	–	NA
Cleft lip/palate	+	NA	–	–	NA	–	NA	–	–	–
Eye/vision anomalies	NA	–	–	–	NA	–	NA	–	–	–
Cutaneous anomalies	+	+	+	–	NA	–	NA	+	+	–
Perinatal complications	+	+	+	–	NA	–	NA	–	–	–
Other	+	–	–	+	NA	+	NA	+	–	–

More information available in the supplemental clinical information document.

ASD, autism spectrum disorder; F, female; M, male; MRI, magnetic resonance imaging; NA, not available.

damaging, score 0.667; MutPred-indel score, 0.33463; MutationTaster2021 benign). Therefore, testing for *HNRNPU* epismutation promoted variant reevaluation and ultimately its reclassification as likely benign.

Screening of an unresolved case using the *HNRNPU* epismutation

Using the SVM classifier constructed in Figure 3C, unresolved cases in the EKD, the database that houses cases, and the DNAm data used by the EpiSign classifier were screened using the *HNRNPU* epismutation. Here, we identified a case (case 10) with an MVP score close to 1 that clustered with *HNRNPU* cases in both hierarchical clustering and MDS plots (Figure 4A and B). Through subsequent follow up

with the submitting clinical center we were able to confirm that the individual carried a variant in *HNRNPU* (NM_031844.2:c.1720_1722del p.(Lys574del)) (Table 1). This variant was not disclosed at the time of original assessment by EpiSign and submission to the EKD, leading this sample to be labeled “unresolved” in the EKD because it was negative for all other detectable epismutations. This variant was labeled as likely pathogenic according to the ACMG guidelines.^{20,21}

To improve the specificity and refine the detected epismutation to be used as a biomarker for the EpiSign test, we repeated the epismutation mapping steps using the 9 confirmed likely pathogenic/pathogenic *HNRNPU* cases (6 previous training cases, 2 validation cases [7 and 8], and 1 unresolved case [10]) because training samples against age and sex matched controls. We retained 106 differentially methylated



Figure 2 Facial appearance of our cases with variants in *HNRNPU*. A and B. Case 1 at 11 months and age 6 years respectively. C. Case 2 at 28 years of age. D. Case 4 at 7 years of age. E. Case 6 at 28 years of age. F and G. Case 7 at 17 years and age 27 years, respectively. H and I. Case 8 at age 6 and age 14 years, respectively.

CpG probes in the final episignature. Results were visualized using the same unsupervised clustering, SVM and cross validation methods (Supplemental Figure 2). Through inclusion of these additional samples we observed stronger specificity and sensitivity with improved MVP scores and clustering results of leave-one-out cross validation.

Genome-wide DNAm profiles of *HNRNPU* samples show an overall increase in DNAm

Next, we assessed genome-wide DNAm changes in individuals with pathogenic *HNRNPU* variants and correlated these to the 56 other episignatures reported by Levy et al.²⁶ Here, we compared genome-wide DNAm profiles of the 9 training cases with episignature-negative, age and sex matched controls from the EKD. We detected a total of 4780 DMPs (false discovery rate < 0.05) that predominantly showed a global hypermethylation profile can be seen in Figure 5 as described below. In the 56 episignatures in the Levy et al study, 66% ($n = 37$) showed hypomethylation, in contrast to 34% ($n = 19$) that showed global hypermethylation (Figure 5).²⁶

Evaluation of the *HNRNPU* episignature compared with that of 56 NDDs

We compared the aforementioned list of DMPs from the *HNRNPU* cohort with the same DMP lists generated by Levy et al for 56 other DNAm profiles on EpiSign.²⁶ Using

a correlation matrix of DMPs showing the percentage of probes shared between each paired cohort, we observed that the DMPs associated with Velocardiofacial syndrome (VCFS) and BAFopathy had the highest overlap with *HNRNPU* (~15%). In addition, the DMPS associated with several other disorders showed overlap with *HNRNPU*, including approximately 13% with Duplication 7q11.23 syndrome (Dup 7) and Luscan-Lumish syndrome (*SETD2*), approximately 12% in CHARGE syndrome (*CHD7*), and approximately 11% in Cornelia de Lange (*NIPBL*, *SMCIA*, *SMC3*, and *RAD21*), Intellectual developmental disorder X-linked 97 (*MRX97*; *ZNF711*), and Intellectual developmental disorder X-linked syndromic Claes-Jensen type (*MRXSCJ*; *KDM5C*) syndromes (Supplemental Figure 3). All other disorders showed a 10% or less overlap. Alternatively, the largest number of *HNRNPU* DMPs are shared with Tatton-Brown-Rahman syndrome (TBRS; *DNMT3A*) approximately 46% and Beck-Fahrner syndrome (BEFAHRS; *TET3*) approximately 45%. These results were also visualized in a circos plot (Figure 6) in which we observed overlap with 55 other disorders. However, no DMP overlap was observed with *KDM4B*.

To determine the relatedness of each of the disorders, we visualized the DMP overlap as well as directionality of the change (hypo or hypermethylation) using a binary tree with each node corresponding to a cohort as described in the methods. Herein, we observed that *HNRNPU* clustered within a hypermethylation branch alongside Beck-Fahrner syndrome (BEFAHRS; *TET3*), *KDM2B*-related syndrome (*KDM2B*), Menke-Hennekam syndromes 1 and 2 (MKHK_ID4;

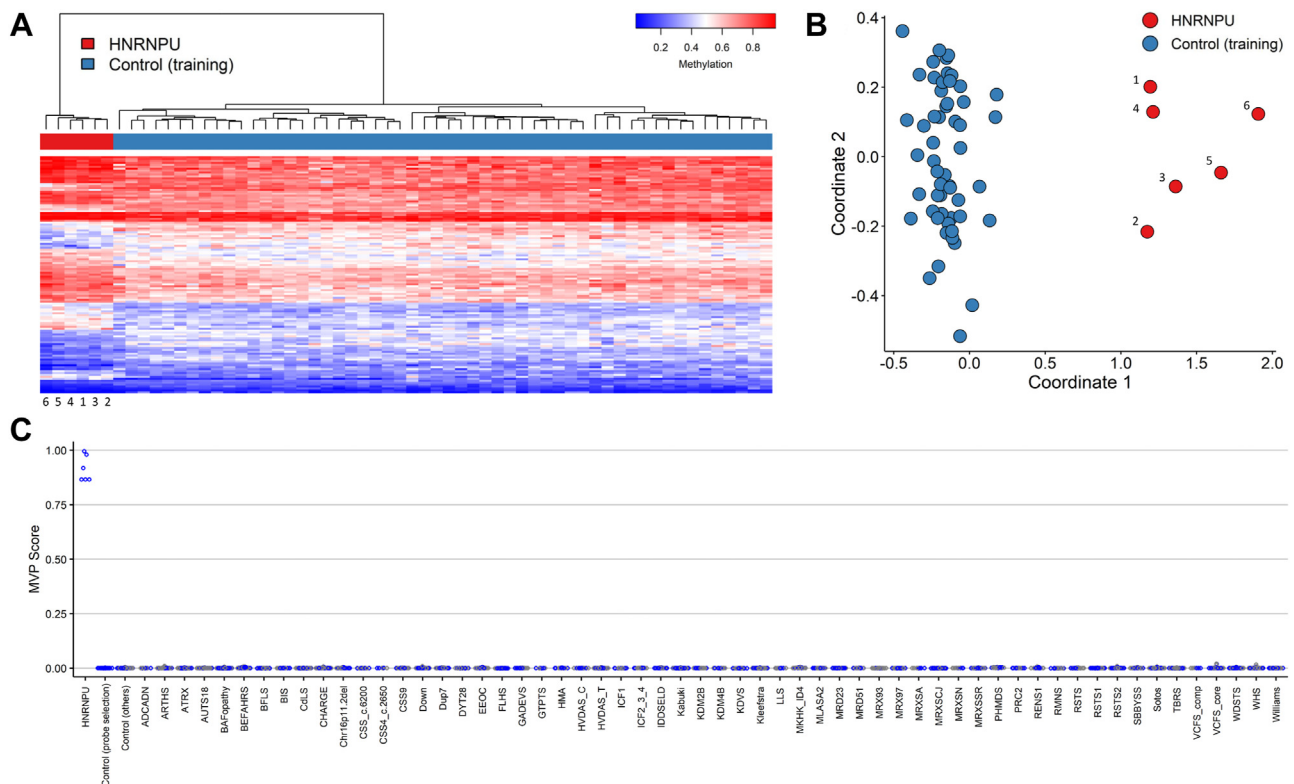


Figure 3 HNRNPU epigenature. A. Heatmap shows clustering of the HNRNPU training cases (red) away from age- and sex-matched controls (blue); each column represents a single case or control sample, and each row represents 1 of the 123 CpG probes selected for the epigenature. B. Multidimensional scaling plot shows clustering of HNRNPU cases from controls. The x- and y-axis represent the first and second dimension of the output (coordinates 1 and 2, respectively). C. Support Vector Machine classifier model, the x-axis represents an epigenature on the EpiSign classifier and the y-axis a probability score, referred to as a methylation variant pathogenicity score (MVP). The model was trained using the 123 selected HNRNPU epigenature probes, and 75% of controls and 75% of other neurodevelopmental/epigenature disorder samples (blue). The remaining 25% controls and 25% of other disorder samples were used for testing (gray). Plot shows the HNRNPU discovery cases with an MVP score close to 1 compared with all other samples that are at or close to 0, showing the specificity of the classifier and epigenature. ADCADN, cerebellar ataxia deafness and narcolepsy syndrome; AUTS18, susceptibility to autism 18; BEFAHRS, Beck-Fahrner syndrome; BFLS, Borjeson-Forsman-Lehmann syndrome; BISS, blepharophimosis intellectual disability SMARCA2 syndrome; CdLS, Cornelia de Lange syndrome; CHARGE, CHARGE syndrome; Chr16p11.2del, chromosome 16p11.2 deletion syndrome; CSS, Coffin-Siris syndrome; CSS4, Coffin-Siris syndrome 4; CSS9, Coffin-Siris syndrome 9; Down, Down syndrome; Dup7, 7q11.23 duplication syndrome; DYT28, Dystonia 28; EEOC, epileptic encephalopathy-childhood onset; FLHS, floating harbour syndrome; GTPTS, genitopatellar syndrome; HMA, Hunter McAlpine craniosynostosis syndrome; HNRNPU, heterogeneous nuclear ribonucleoprotein U; HVDAS: Helmsmoortel-van der Aa syndrome; ICF, immunodeficiency-centromeric instability-facial anomalies syndrome; IDDSELD, intellectual developmental disorder with seizures and language delay; Kabuki, Kabuki syndrome; KDVS, Koolen-De Vries syndrome; Kleefstra, Kleefstra syndrome; LLS, Luscan-Lumish syndrome; MKHK, Menke-Hennekam syndrome; MLASA2, myopathy lactic acidosis and sideroblastic anemia 2; MRD23, intellectual developmental disorder 23; MRD51, intellectual developmental disorder 51; MRX93, intellectual developmental disorder X-linked 93; MRX97, intellectual developmental disorder X-linked 97; MRXSA, intellectual developmental disorder X-linked syndromic Armfield type; MRXSCH, intellectual developmental disorder X-linked syndromic Christianson type; MRXSCJ, intellectual developmental disorder X-linked syndromic Claes-Jensen type; MRXSN, intellectual developmental disorder X-linked syndromic Nascimento type; MRXSSR, intellectual developmental disorder X-linked syndromic Snyder-Robinson type; PHMDS, Phelan-McDermid syndrome; PRC2, PRC2 complex (Weaver and Cohen-Gibson) syndrome; RENS1, Renpenning syndrome; RMNS, Rahman syndrome; RSTS, Rubinstein-Taybi syndrome; SBBYSS, Ohdo syndrome; Sotos, Sotos syndrome; TBRS, Tatton-Brown-Rahman syndrome; WDSTS, Wiedemann-Steiner syndrome; WHS, Wolf-Hirschhorn syndrome; Williams, Williams syndrome.

CREBBP and *EP300*), Kabuki syndromes 1 and 2 (Kabuki; *KMT2D* and *KDM6A*), Intellectual developmental disorder autosomal dominant 23 (MRD23; *SETD5*), BAFopathy, and Coffin-Siris syndrome-9 (CSS9; *SOX11*) (Figure 7). These shared DMPs may indicate that common underlying biological processes are affected in each disorder because of overlap in functional consequences to the epigenome.

Lastly, we annotated the genomic locations of all the DMPs for all 57 cohorts in relation to genes and CGIs. This analysis demonstrated that the *HNRNPU* DMPs predominantly map within coding regions of genes (Figure 8A) and almost equally in CpG island shore regions (within 0-2 kb of a CpG island boundary) and regions outside of CGIs (Figure 8B). Similar to other disorders with epigenatures, *HNRNPU* DMPs also map

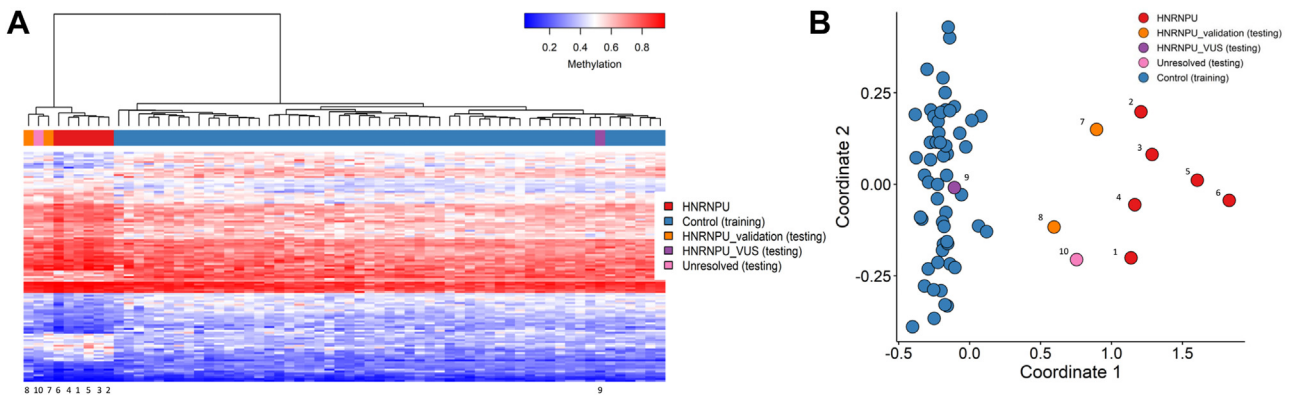


Figure 4 Validation of the HNRNPU episignature. A. Heatmap. Each column represents a single HNRNPU case or control, and each row represents 1 of the 123 CpG probes selected for the episignature. This heatmap shows clustering of the 2 HNRNPU validation cases (orange) and a previously unresolved case (pink) with the 6 HNRNPU training cases (red) from controls (blue). The VUS sample (purple) is shown to cluster with controls. B. Multidimensional scaling plot confirming the clustering of all pathogenic HNRNPU cases (training and validation) from controls. X- and y-axis represent the first and second dimension of the output (coordinates 1 and 2, respectively). HNRNPU, heterogeneous nuclear ribonucleoprotein U; VUS, variant of uncertain significance

to intergenic regions. We also observed a difference in the distribution of DMPs in the *HNRNPU* profile compared with the background probe distribution in relation to genes (P value $< 2.29 \times 10^{-151}$) and CGIs (P value $< 2.53 \times 10^{-225}$). The *HNRNPU* DMPs were located more in promoter and promoter+ regions than the background probes (Figure 8A). In relation to CGIs, the *HNRNPU* DMPs were located more in CGIs and shores and less in inter-CGI regions compared with background (Figure 8B).

Differentially methylated regions (DMRs)

We identified 18 DMRs (Supplemental Table 2), of which 12 were hypermethylation events (67%) and 6 demonstrated hypomethylation (33%). This is in line with the overall global mean methylation difference (Figure 5). Twelve DMRs were in regions with CGIs (67%) (Supplemental Figure 4), 9 of these were hypermethylation events and 3 hypomethylation. Additionally, 8 DMRs (44%) were annotated to predicted

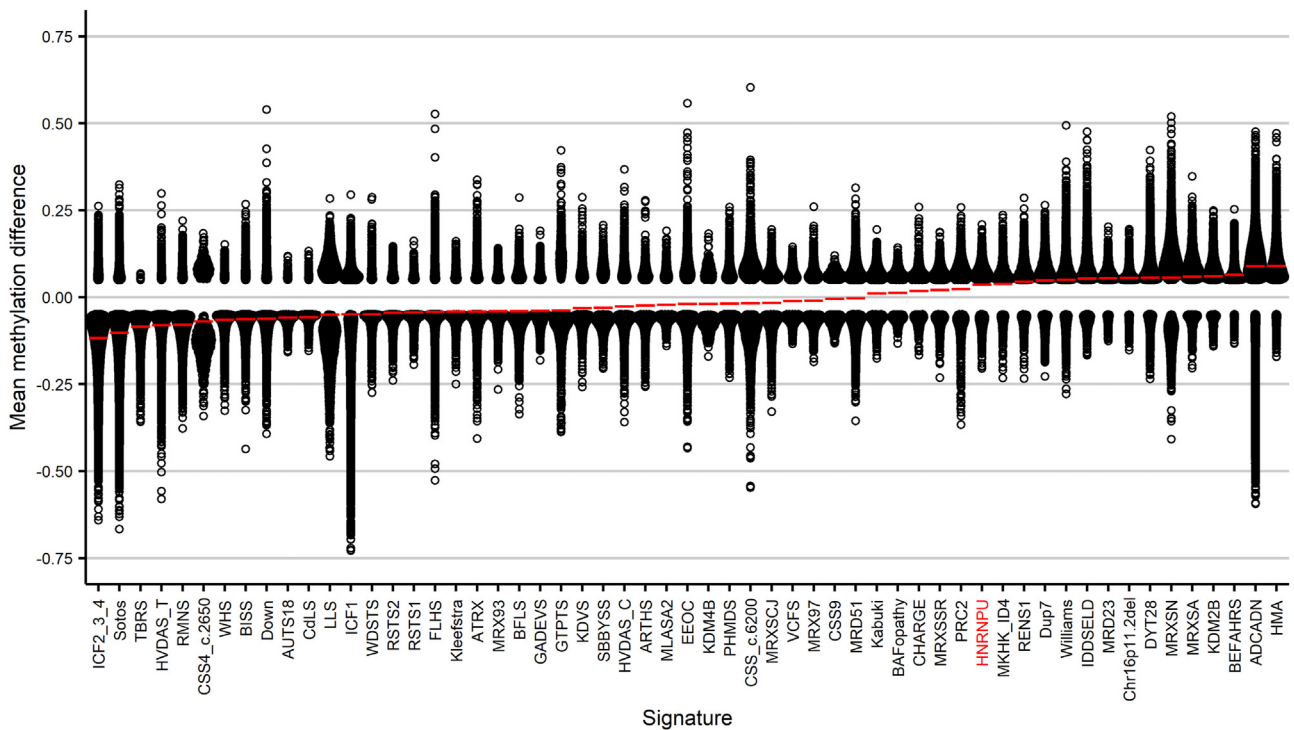


Figure 5 Genome-wide DNA methylation profiles of the HNRNPU cohort and 56 episignatures on EpiSign. Global methylation differences of all differentially methylated probes (FDR < 0.05) for each cohort, sorted by mean methylation. Each circle represents 1 probe. Red lines indicate mean methylation. The x-axis represents 1 of the 57 episignatures and the y-axis is the mean methylation difference. FDR, false discovery rate; HNRNPU, heterogeneous nuclear ribonucleoprotein U.

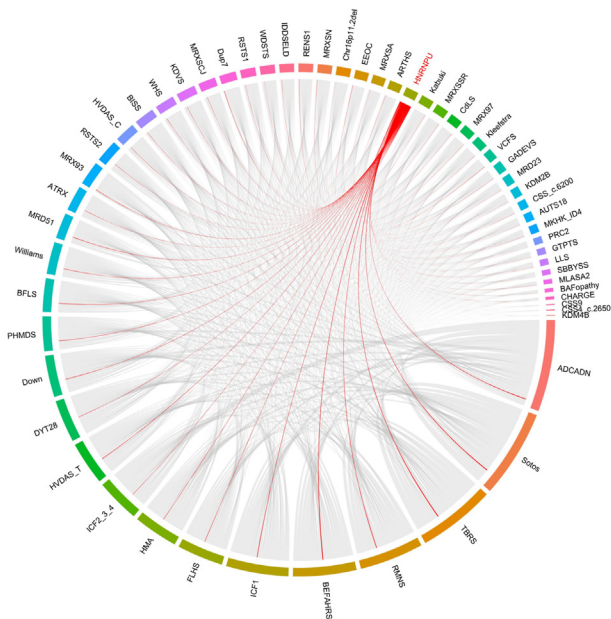


Figure 6 DMPs shared between the *HNRNPU* cohort and 56 other epismutants on EpiSign. Circos plot representing the probes shared between each pair of cohorts. The thickness of the connecting lines indicates the number of probes shared between the 2 cohorts. *HNRNPU* connections are highlighted in red. DMP, differentially methylated probe; *HNRNPU*, heterogeneous nuclear ribonucleoprotein U.

promoters with TSSs, 7 of these were in regions with CGIs. Nine DMRs mapped to enhancers (50%) and 5 mapped to regions with no predicted regulatory elements (28%). Two of the DMRs (11%) were predicted to overlap CCCTC-binding factor binding sites that are suggestive of possible disruption to chromatin loop formation and topologically associated domains associated with these regions. Five of the DMRs were located on chromosome 19 (28%); 2 DMRs each on chromosomes 1, 2, and 13 (11% each); and 1 DMR on chromosomes 4, 5, 9, 11, 14, 16, and 22. One hypermethylated DMR containing an enhancer and CCCTC-binding factor binding site overlaps the *CHKB* gene that is associated with congenital muscular dystrophy megaconial type (OMIM #602541) (Supplemental Figure 4). This disorder shares several phenotypic manifestations similar to DEE54, including microcephaly, hypotonia, ID, delayed motor development, poor speech, and seizures.

Discussion

Aberrant DNAm patterns as a consequence of genetic defects are thought to be established during early embryonic development and can be detected in all tissues, including blood, making them easily accessible as biomarkers in clinical diagnostics.¹¹ These biomarkers, or epismutants, associated with a given Mendelian NDD can be helpful in diagnosing unsolved cases with unexplained ID and to reclassify VUS.^{25,35,36}

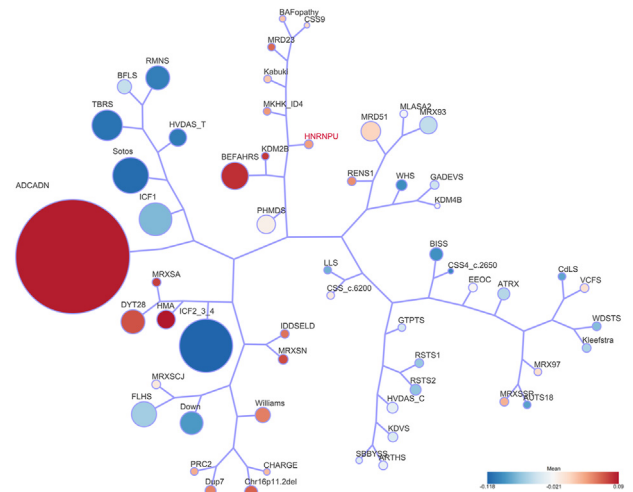


Figure 7 Tree and leaf visualization of Euclidean clustering of all 57 cohorts using the top 500 DMPs for each group (for cohorts with less than 500 DMPs all DMPs were used). Cohort samples were aggregated using the median value of each probe within a group. A leaf node represents a cohort, with node sizes illustrating relative scales of the number of selected DMPs for the corresponding cohort, and node colors are indicative of the global mean methylation difference (ie, the overall methylation trend, hypomethylation [blue] or hypermethylation [red]). DMP, differentially methylated probe.

The aim of this study was to detect and validate a DNAm epismutant for cases with *HNRNPU* variants and to further explore the potential functional overlap with other Mendelian disorders that have known epismutants. We describe a specific DNAm epismutant for likely pathogenic/pathogenic heterozygous *HNRNPU* variants. We assessed DNAm profiles from peripheral blood of 8 individuals with confirmed likely pathogenic/pathogenic variants in *HNRNPU*, including SNVs and deletions spanning *HNRNPU*. The classification model was built with cases with confirmed likely pathogenic/pathogenic variants and later validated in a separate cohort. During cross-validation of the final epismutant, which incorporated previous training cohort and validation samples, all the cases clustered together and away from unaffected controls, demonstrating that this *HNRNPU* epismutant is robust and reproducible. The SVM model confirmed that the selected epismutant probes represented a strong biomarker for the molecular diagnosis of DEE54. This model indicates the *HNRNPU* epismutant is highly specific and sensitive and unique when compared with the epismutants of other EpiSign NDDs.

As epismutants have been shown to aid in the reclassification of VUS,³⁷ we tested an individual with an *HNRNPU* VUS NM_031844.2:c.837_839del p.(Glu279del) (case 9) to determine if it mapped to the *HNRNPU* epismutant. The classification scores that were applied for this variant were PS2 (de novo) and PM4 (length changes as a result of in-frame deletions/insertions in a nonrepeat region or stop-loss

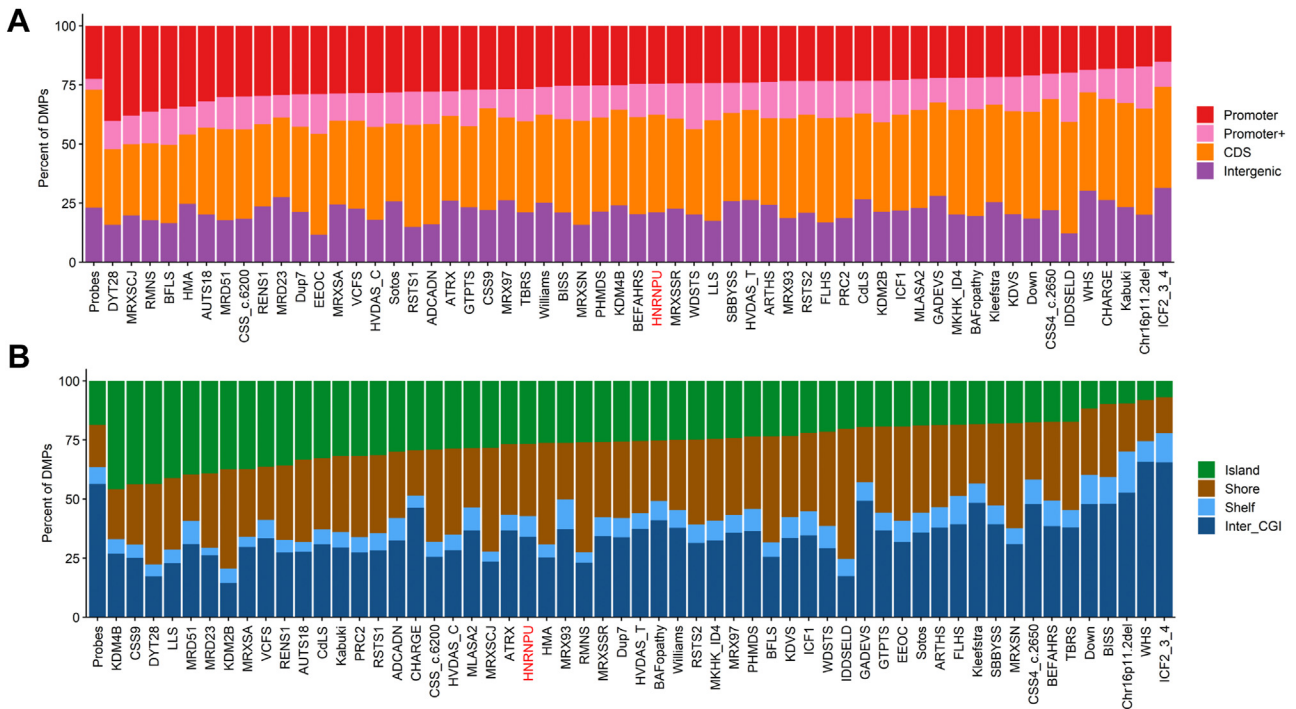


Figure 8 DMPs of HNRNPU cohort (red) and 56 other epismutations on EpiSign. X-axis represents 1 of the 57 epismutations (HNRNPU + 56 EpiSign) and the y-axis the percentage of DMPs. A. DMPs annotated in the context of genes. Promoter, 0 to 1 kb upstream of the TSS; Promoter+, 1 to 5 kb upstream of the TSS; CDS, coding sequence; Intergenic, all other regions of the genome. B. DMPs annotated in the context of CpG islands. Island, CpG islands; Shore, within 0 to 2 kb of a CpG island boundary; Shelf, within 2 to 4 kb of a CpG island boundary; inter-CGI, all other regions in the genome. The Probes column in panels A and B represents the background distribution determined in the study by Levy et al¹² of all array probes after initial filtering and used as input for DMP analysis. CDS, coding sequence; DMP, differentially methylated probe; HNRNPU, heterogeneous nuclear ribonucleoprotein U; TSS, transcription start site.

variants), which makes the variant likely pathogenic. However, the classification score BS2 (observed in a healthy adult individual for a recessive [homozygous], dominant [heterozygous], or X-linked [hemizygous] disorder, with full penetrance expected at an early age) was also applied and the phenotype of this patient was not *HNRNPU* typically; therefore, it was classified as a VUS. The methylation profile did not cluster together within the *HNRNPU* cases in the MDS plot and yielded an MVP score near zero, indicating the absence of an *HNRNPU* epismutation. The absence of a gene-specific methylation pattern is not conclusive evidence of a benign genetic variant but does strongly support that hypothesis.¹⁶ This resulted in the re-evaluation of the p.(Glu279del) variant, with the in silico predictions of pathogenicity for this variant being unable to corroborate *HNRNPU* loss-of-function. Moreover, the variant was found twice in the heterozygous state in the Genome Aggregation Database, in which it is expected that no individuals with a clear neurodevelopmental phenotype are included. Based on these results, we suggest that the p.(Glu279del) VUS can be reclassified as benign and is likely not the cause of the phenotype observed in case 9. Further testing and research is needed for this variant and case.

Then the SVM classifier was applied to the unresolved cases in the EKD. Cases are labeled unresolved in the EKD when they do not match any of the current detectable

epismutations. We identified 1 case (case 10) with an MVP score close to 1 that clustered with the *HNRNPU* cases in both hierarchical clustering and MDS plots. After contacting the clinical center, we were able to confirm that an *HNRNPU* variant was subsequently found after ES and the phenotype of this individual fit with DEE54. The variant; NM_031844.2:c.1720_1722delAAG p.(Lys574del) was also classified as likely pathogenic according to the ACMG guidelines.²⁰ This study establishes *HNRNPU* epismutation as a powerful tool that can be applied in the screening of patients with NDD, as a reflex test for unsolved patients as well as in variant interpretation.¹⁶

This cohort included 2 individuals with large CNVs (case 5 and 6) involving multiple genes in addition to *HNRNPU*. Those individuals were diagnosed with autosomal dominant intellectual developmental disorder 22 also named chromosome 1q43-q44 deletion syndrome (OMIM 612337). However, both cases clustered together with individuals carrying deleterious SNVs in *HNRNPU*. Case 5 involves a deletion of 7 Mb, involving *ZBTB18* (OMIM 608433), 1 of the candidate genes for the NDD phenotype in 1q43-q44 deletion syndrome (OMIM #612337).¹⁸ Case 6 had a smaller deletion; however, it did not encompass *ZBTB18*. Taken together, this may indicate that *HNRNPU* is one of the syndrome-causing genes in the 1q43-q44 deletion region^{1,18,38,39} and that the aberrant methylation is mostly

driven by *HNRNPU*. *HNRNPU* has been identified as the main candidate for the epilepsy phenotype observed in individuals with 1q43-q44 deletion syndrome,¹⁸ and ES analysis demonstrated that *HNRNPU* variants are also responsible for the neurodevelopmental phenotypes.⁴⁰

We identified 18 DMRs that were predominantly hypermethylation events. Nine hypermethylation events occurred across CGIs in regions containing predicted promoters or enhancers. Hypermethylation of a region containing a CpG island, a predicted enhancer, as well as the *CHKB* gene, was observed. *CHKB* is associated with congenital muscular dystrophy megaconial type (OMIM #602541), a disorder with several overlapping clinical features with DEE54 including microcephaly, hypotonia, ID, delayed motor development, poor speech, and seizures. Generally, it is postulated that hypermethylated promoter regions lead to decreased gene expression and thus decreased protein levels, which is possibly leading to overlapping clinical features with DEE54. Earlier research by *Haghshenas et al* also showed a DMR involving *CHKB* in X-linked syndromic ID Armfield type. Here, *CHKB* was also hypermethylated and overlapping with the phenotype.⁴¹ Hypermethylation was also observed across the predicted promoters of several other genes that are currently not associated with Mendelian disorders. Further work would be required to investigate the potential contribution of these regions and genes to the pathological mechanisms in DEE54.

When we compared the DMPs of the previously mapped disorders on EpiSign, the global *HNRNPU* DNAm profile showed high overlap with the VCFS and BAFopathy cohorts. Another study showed that cells carrying *HNRNPR* variants, another gene of the hnRNP family, demonstrated overexpression of *TBX1*; a gene encompassed in the critical region of VCFS.⁴² Other groups have shown that *BRM* and *BRG1*, (aliases *SMARCA2* and *SMARCA4*),⁴³ important subunits of SWI/SNF complex, are involved with splicing machinery through interactions with several RNA binding factors, such as hnRNP.⁴⁴ These studies provide possible hypotheses regarding the functional implications of the observed DMP overlap between *HNRNPU* and the genes involved in VCFS or BAF complexes observed in this study. Examining the directionality of the *HNRNPU* methylation changes and their similarity to the hypermethylated branch in Figure 7, including BEFAHRS (*TET3*) and *KDM2B*, provides limited insight into functional overlap as all disorder related genes are involved in epigenetic regulation/machinery. Given that the epigenetic machinery must work together in a carefully orchestrated way, downstream effects of mutations in different genes may affect similar methylation loci, resulting in pleiotropic effects that are difficult to delineate.⁴⁵ Further investigations are required to better understand how these similarities in DNAm changes translate into phenotypic consequences.

A possible limitation of this study is the relatively small sample size. Because of the rarity of Mendelian NDDs, episignatures are established first using a small number of

affected individuals.^{12,46} Future cases with *HNRNPU* variants need to be analyzed to increase the sensitivity and specificity of the *HNRNPU* episignature. Additionally, further cases with differing CNVs may result in the detection of possible nested signatures, or subsignatures, related to differences in genes within the deletion region with epigenetic functions.

Conclusion

In this study we show a specific and sensitive DNAm episignature for individuals carrying pathogenic variants in *HNRNPU* or a CNV that includes *HNRNPU*. This new diagnostic tool can be used to screen for DEE54 and reclassify variants in *HNRNPU* as pathogenic or prompt re-evaluation of a variant as benign. This additional testing may help patients and their families to end an (often) long diagnostic odyssey. Global DNAm changes in individuals with *HNRNPU* variants provide insights into the molecular pathways affected by downstream epigenetic disruptions in this disorder and may eventually lead to personalized treatment for this NDD based on identified pathological mechanisms.

Data Availability

Raw DNA methylation data are available from the authors on request.

Acknowledgments

The authors would like to thank the participants and their families described in this study.

Funding

Funding for this study is provided in part by the Government of Canada through Genome Canada and the Ontario Genomics Institute (OGI-188) and Ministero dell'Istruzione, dell'Università e della Ricerca (MIUR) PRIN2020 code 20203P8C3X.

Author Information

Conceptualization: K.R., L.v.d.L., M.A., M.M.A.M.M., B.S., M.M.v.H., P.H.; Data Curation: K.R., L.v.d.L., S.H., R.R., M.A.L.; Formal Analysis: K.R., L.v.d.L., S.H., R.R., M.A.L.; Investigation: L.v.d.L., S.T., N.V., P.L., N.B.-P., G.T., C.M., B.K., T.B.d.V., C.M.L.V.-T., N.V., J.J.v.d.S., R.O., A.B., G.B.F., M.M.-I., R.H., M.A., M.M.v.H.; Methodology: K.R., M.M.A.M.M., B.S., P.H., M.M.v.H.;

Project Administration: M.M.A.M.M., B.S., M.M.v.H., P.H.; Supervision: M.M.A.M.M., B.S., M.M.v.H., P.H.; Validation: K.R., L.v.d.L.; Visualization: K.R., L.v.d.L.; Writing-original draft: K.R., L.v.d.L.; Writing-review and editing: K.R., L.v.d.L., S.T., P.L., R.H., M.M.A.M.M., B.S., M.M.v.H., P.H.

Ethics Declaration

The study was conducted in accordance with the regulations of the Western University Research Ethics Board (REB116108 and REB106302) and The Medical Ethical Committee (METC) of the Amsterdam UMC, location AMC. METC approval (anonymous study, further study in line with a clinical question). We obtained written informed consent from the participants or their substitute decision maker to publish patients' clinical and genetic information. Explicit consent for the publication of individuals' photographs was obtained separately.



Conflict of Interest

The authors declare no conflicts of interest.

Additional Information

The online version of this article (<https://doi.org/10.1016/j.gim.2023.100871>) contains supplementary material, which is available to authorized users.

Authors

Kathleen Rooney^{1,2}, Liselot van der Laan³ , Slavica Trajkova⁴, Sadegheh Haghshenas¹, Raissa Relator¹, Peter Lauffer³, Niels Vos³, Michael A. Levy¹, Nicola Brunetti-Pierrri^{5,6}, Gaetano Terrone⁶, Cyril Mignot⁷, Boris Keren⁷, Thierry B. de Villemeur⁸, Catharina M.L. Volker-Touw⁹, Nienke Verbeek⁹, Jasper J. van der Smagt⁹, Renske Oegema⁹, Alfredo Brusco^{4,10}, Giovanni B. Ferrero¹¹, Mala Misra-Isrie³, Ron Hochstenbach³, Mariëlle Alders³, Marcel M.A.M. Mannens³, Bekim Sadikovic^{1,2,*} , Mieke M. van Haelst³, Peter Henneman^{3,*}

Affiliations

¹Verspeeten Clinical Genome Centre, London Health Science Centre, London, ON, Canada; ²Department of Pathology and Laboratory Medicine, Western University, London, ON, Canada; ³Department of Human Genetics,

Amsterdam Reproduction and Development Research Institute, Amsterdam University Medical Centers, University of Amsterdam, Amsterdam, The Netherlands; ⁴Department of Medical Sciences, University of Torino, Torino, Italy; ⁵Telethon Institute of Genetics and Medicine (TIGEM), Pozzuoli, Italy; ⁶Department of Translational Medicine, Federico II University, Naples, Italy; ⁷Assistance Publique-Hopitaux de Paris, Sorbonne Université, Département de Génétique, Groupe Hospitalier Pitie-Salpetriere et Hopital Trousseau, Paris, France; ⁸Sorbonne Université, APHP, Hôpital Trousseau, Service de neuro-pédiatrie, Paris, France; ⁹Department of Genetics, University Medical Centre Utrecht, Utrecht University, Utrecht, The Netherlands; ¹⁰Medical Genetics Unit, Città della Salute e della Scienza University Hospital, Torino, Italy; ¹¹Department of Clinical and Biological Science, University of Torino, Torino, Italy

References

1. Bramswig NC, Lüdecke HJ, Hamdan FF, et al. Heterozygous HNRNPU variants cause early onset epilepsy and severe intellectual disability. *Hum Genet.* 2017;136(7):821-834. <http://doi.org/10.1007/s00439-017-1795-6>
2. Taylor J, Spiller M, Ranguin K, et al. Expanding the phenotype of HNRNPU-related neurodevelopmental disorder with emphasis on seizure phenotype and review of literature. *Am J Med Genet A.* 2022;188(5):1497-1514. <http://doi.org/10.1002/ajmg.a.62677>
3. Wu B, Su S, Patil DP, et al. Molecular basis for the specific and multivalent recognitions of RNA substrates by human hnRNP A2/B1. *Nat Commun.* 2018;9(1):420. <http://doi.org/10.1038/s41467-017-02770-z>
4. Lim I, Jung Y, Kim DY, Kim KT. HnRNP Q Has a suppressive role in the translation of mouse Cryptochrome1. *PLoS One.* 2016;11(7):e0159018. <http://doi.org/10.1371/journal.pone.0159018>
5. Geuens T, Bouhy D, Timmerman V. The hnRNP family: insights into their role in health and disease. *Hum Genet.* 2016;135(8):851-867. <http://doi.org/10.1007/s00439-016-1683-5>
6. Sapir T, Kshirsagar A, Gorelik A, et al. Heterogeneous nuclear ribonucleoprotein U (HNRNPU) safeguards the developing mouse cortex. *Nat Commun.* 2022;13(1):4209. <http://doi.org/10.1038/s41467-022-31752-z>
7. Yugami M, Okano H, Nakanishi A, Yano M. Analysis of the nucleocytoplasmic shuttling RNA-binding protein HNRNPU using optimized HITS-CLIP method. *PLoS One.* 2020;15(4):e0231450. <http://doi.org/10.1371/journal.pone.0231450>
8. Zhang L, Song D, Zhu B, Wang X. The role of nuclear matrix protein HNRNPU in maintaining the architecture of 3D genome. *Semin Cell Dev Biol.* 2019;90:161-167. <http://doi.org/10.1016/j.semcdb.2018.07.006>
9. Bjornsson HT. The Mendelian disorders of the epigenetic machinery. *Genome Res.* 2015;25(10):1473-1481. <http://doi.org/10.1101/gr.190629.115>
10. Fahrner JA, Bjornsson HT. Mendelian disorders of the epigenetic machinery: tipping the balance of chromatin states. *Annu Rev Genomics Hum Genet.* 2014;15:269-293. <http://doi.org/10.1146/annurev-genom-090613-094245>
11. Sadikovic B, Aref-Eshghi E, Levy MA, Rodenhiser D. DNA methylation signatures in Mendelian developmental disorders as a diagnostic bridge between genotype and phenotype. *Epigenomics.* 2019;11(5):563-575. <http://doi.org/10.2217/epi-2018-0192>

12. Levy MA, McConkey H, Kerkhof J, et al. Novel diagnostic DNA methylation epismutations expand and refine the epigenetic landscapes of Mendelian disorders. *HGG Adv.* 2022;3(1):100075. <http://doi.org/10.1016/j.xhgg.2021.100075>
13. Rooney K, Levy MA, Haghshenas S, et al. Identification of a DNA methylation epismutation in the 22q11.2 deletion syndrome. *Int J Mol Sci.* 2021;22(16):8611. <http://doi.org/10.3390/ijms22168611>
14. Rooney K, Sadikovic B. DNA methylation epismutations in neurodevelopmental disorders associated with large structural copy number variants: clinical implications. *Int J Mol Sci.* 2022;23(14):7862. <http://doi.org/10.3390/ijms23147862>
15. van der Laan L, Rooney K, Trooster TM, Mannens MM, Sadikovic B, Henneman P. DNA methylation epismutations: insight into copy number variation. *Epigenomics.* 2022;14(21):1373-1388. <http://doi.org/10.2217/epi-2022-0287>
16. Aref-Eshghi E, Rodenhiser DI, Schenkel LC, et al. Genomic DNA methylation signatures enable concurrent diagnosis and clinical genetic variant classification in neurodevelopmental syndromes. *Am J Hum Genet.* 2018;102(1):156-174. <http://doi.org/10.1016/j.ajhg.2017.12.008>
17. Balasubramanian M. HNRNPU-related neurodevelopmental disorder. In: Adam MP, Everman DB, Mirzaa GM, et al, editors. *GeneReviews*(®). University of Washington; 1993-2023.
18. Depienne C, Nava C, Keren B, et al. Genetic and phenotypic dissection of 1q43q44 microdeletion syndrome and neurodevelopmental phenotypes associated with mutations in ZBTB18 and HNRNPU. *Hum Genet.* 2017;136(4):463-479. <http://doi.org/10.1007/s00439-017-1772-0>
19. Durkin A, Albaba S, Fry AE, et al. Clinical findings of 21 previously unreported probands with HNRNPU-related syndrome and comprehensive literature review. *Am J Med Genet A.* 2020;182(7):1637-1654. <http://doi.org/10.1002/ajmg.a.61599>
20. Richards S, Aziz N, Bale S, et al. Standards and guidelines for the interpretation of sequence variants: a joint consensus recommendation of the American College of Medical Genetics and Genomics and the Association for Molecular Pathology. *Genet Med.* 2015;17(5):405-424. <http://doi.org/10.1038/gim.2015.30>
21. Riggs ER, Andersen EF, Cherry AM, et al. Technical standards for the interpretation and reporting of constitutional copy-number variants: a joint consensus recommendation of the American College of Medical Genetics and Genomics (ACMG) and the Clinical Genome Resource (ClinGen). *Genet Med.* 2020;22(2):245-257. <http://doi.org/10.1038/s41436-019-0686-8>
22. Vaser R, Adusumalli S, Leng SN, Sikic M, Ng PC. SIFT missense predictions for genomes. *Nat Protoc.* 2016;11(1):1-9. <http://doi.org/10.1038/nprot.2015.123>
23. Pagel KA, Antaki D, Lian A, et al. Pathogenicity and functional impact of non-frameshifting insertion/deletion variation in the human genome. *PLoS Comput Biol.* 2019;15(6):e1007112. <http://doi.org/10.1371/journal.pcbi.1007112>
24. Steinhaus R, Proft S, Schuelke M, Cooper DN, Schwarz JM, Seelow D. MutationTaster2021. *Nucleic Acids Res.* 2021;49(W1):W446-W451. <http://doi.org/10.1093/nar/gkab266>
25. van der Laan L, Rooney K, Alders M, et al. Epismutation mapping of TRIP12 provides functional insight into Clark-Baraitser syndrome. *Int J Mol Sci.* 2022;23(22):13664. <http://doi.org/10.3390/ijms232213664>
26. Levy MA, Relator R, McConkey H, et al. Functional correlation of genome-wide DNA methylation profiles in genetic neurodevelopmental disorders. *Hum Mutat.* 2022;43(11):1609-1628. <http://doi.org/10.1002/humu.24446>
27. Aryee MJ, Jaffe AE, Corrada-Bravo H, et al. Minfi: a flexible and comprehensive Bioconductor package for the analysis of Infinium DNA methylation microarrays. *Bioinformatics.* 2014;30(10):1363-1369. <http://doi.org/10.1093/bioinformatics/btu049>
28. Ho DE, Imai K, King G, Stuart EA. MatchIt: nonparametric pre-processing for parametric causal inference. *J Stat Softw.* 2011;42(8):1-28. <http://doi.org/10.18637/jss.v042.i08>
29. Ritchie ME, Phipson B, Wu D, et al. limma powers differential expression analyses for RNA-seq and microarray studies. *Nucleic Acids Res.* 2015;43(7):e47. <http://doi.org/10.1093/nar/gkv007>
30. Houseman EA, Accomando WP, Koestler DC, et al. DNA methylation arrays as surrogate measures of cell mixture distribution. *BMC Bioinformatics.* 2012;13:86. <http://doi.org/10.1186/1471-2105-13-86>
31. Peters TJ, Buckley MJ, Statham AL, et al. De novo identification of differentially methylated regions in the human genome. *Epigenetics Chromatin.* 2015;8:6. <http://doi.org/10.1186/1756-8935-8-6>
32. Gu Z, Gu L, Eils R, Schlesner M, Brors B. circlize implements and enhances circular visualization in R. *Bioinformatics.* 2014;30(19):2811-2812. <http://doi.org/10.1093/bioinformatics/btu393>
33. Cavalcante RG, Sartor MA. Annotatr: genomic regions in context. *Bioinformatics.* 2017;33(15):2381-2383. <http://doi.org/10.1093/bioinformatics/btx183>
34. Kent WJ, Sugnet CW, Furey TS, et al. The human genome browser at UCSC. *Genome Res.* 2002;12(6):996-1006. <http://doi.org/10.1101/gr.229102>
35. Aref-Eshghi E, Bend EG, Colaiacovo S, et al. Diagnostic utility of genome-wide DNA methylation testing in genetically unsolved individuals with suspected hereditary conditions. *Am J Hum Genet.* 2019;104(4):685-700. <http://doi.org/10.1016/j.ajhg.2019.03.008>
36. Bend EG, Aref-Eshghi E, Everman DB, et al. Gene domain-specific DNA methylation epismutations highlight distinct molecular entities of ADNP syndrome. *Clin Epigenet.* 2019;11(1):64. <http://doi.org/10.1186/s13148-019-0658-5>
37. Sadikovic B, Levy MA, Kerkhof J, et al. Clinical epigenomics: genome-wide DNA methylation analysis for the diagnosis of Mendelian disorders. *Genet Med.* 2021;23(6):1065-1074. <http://doi.org/10.1038/s41436-020-01096-4>
38. van der Schoot V, de Munnik S, Venselaar H, et al. Toward clinical and molecular understanding of pathogenic variants in the ZBTB18 gene. *Mol Genet Genom Med.* 2018;6(3):393-400. <http://doi.org/10.1002/mgg3.387>
39. Caliebe A, Kroes HY, van der Smagt JJ, et al. Four patients with speech delay, seizures and variable corpus callosum thickness sharing a 0.440-Mb deletion in region 1q44 containing the HNRNPU gene. *Eur J Med Genet.* 2010;53(4):179-185. <http://doi.org/10.1016/j.ejmg.2010.04.001>
40. Zhu X, Petrovski S, Xie P, et al. Whole-exome sequencing in undiagnosed genetic diseases: interpreting 119 trios. *Genet Med.* 2015;17(10):774-781. <http://doi.org/10.1038/gim.2014.191>
41. Haghshenas S, Levy MA, Kerkhof J, et al. Detection of a DNA methylation signature for the intellectual developmental disorder, X-linked, syndromic, Armfield type. *Int J Mol Sci.* 2021;22(3):1111. <http://doi.org/10.3390/ijms22031111>
42. Duijkers FA, McDonald A, Janssens GE, et al. HNRNPR variants that impair homeobox gene expression drive developmental disorders in humans. *Am J Hum Genet.* 2019;104(6):1040-1059. <http://doi.org/10.1016/j.ajhg.2019.03.024>
43. Centore RC, Sandoval GJ, Soares LMM, Kadoch C, Chan HM. Mammalian SWI/SNF chromatin remodeling complexes: emerging mechanisms and therapeutic strategies. *Trends Genet.* 2020;36(12):936-950. <http://doi.org/10.1016/j.tig.2020.07.011>
44. Gañez-Zapater A, Mackowiak SD, Guo Y, et al. The SWI/SNF subunit BRG1 affects alternative splicing by changing RNA binding factor interactions with nascent RNA. *Mol Genet Genomics.* 2022;297(2):463-484. <http://doi.org/10.1007/s00438-022-01863-9>
45. Greenberg MVC, Bourc'his D. The diverse roles of DNA methylation in mammalian development and disease. *Nat Rev Mol Cell Biol.* 2019;20(10):590-607. <http://doi.org/10.1038/s41580-019-0159-6>
46. Verberne EA, van der Laan L, Haghshenas S, et al. DNA methylation signature for JARID2-neurodevelopmental syndrome. *Int J Mol Sci.* 2022;23(14):8001. <http://doi.org/10.3390/ijms23148001>